

System-Level Performance of Spread Spectrum-Based Add-on Service Overlaid onto the Existing Terrestrial Digital Multimedia Broadcast Band

Seokhyun Yoon, Bo-mi Lim, and Yong Tae Lee

We consider an overlaid broadcast service, where a spread spectrum (SS)-based broadcast signal is overlaid onto the existing terrestrial Digital Multimedia Broadcasting (T-DMB) band. The system is similar to the augmented data transmission in the ATSC DTV, for which it was investigated mostly in terms of link level performance, such as bit error rate. Our focus in this paper is on the system-level performances. More specifically, utilizing both a large scale path loss and a small scale fading channel model, the primary objective is to explore the tradeoff between the coverage and the achievable rate of the overlaid service and, finally, to determine the achievable rate in the overlaid service for marginal coverage reduction in the existing broadcast service. The analytical and simulation results show that an SS-based add-on service of 10 kbps to 20 kbps can co-exist with the T-DMB service while resulting in only a marginal degradation in T-DMB coverage (for example, less than one percent reduction).

Keywords: Digital Multimedia Broadcast (DMB), service overlay, spread spectrum.

Manuscript received Nov. 8, 2011, revised Feb. 23, 2012; accepted Feb. 16, 2012.

This work was supported by the Korea Communications Commission (KCC) under the R&D program supervised by the Korea Communications Agency (KCA) (KCA-2011-11912-02002) and partly by 2010 Dankook University Project for funding RICT.

Seokhyun Yoon (phone: +82 31 8005 3635, syoon@dku.edu) is with the Department of Electronics Engineering, Dankook University, Yongin, Gyeonggi-do, Rep. of Korea.

Bo-mi Lim (blim_vrossi46@etri.re.kr) and Yong Tae Lee (ytle@etri.re.kr) are with the Broadcasting & Telecommunications Convergence Research Laboratory, ETRI, Daejeon, Rep. of Korea.

<http://dx.doi.org/10.4218/etrij.12.0111.0700>

I. Introduction

Nowadays, frequency resources are very scarce, especially the bands below several hundred MHz where an electromagnetic wave travels longer than in higher frequency bands making it suitable for nationwide broadcast services. Frequency resources are also very expensive, and licensing a new band may involve high costs. A popular solution to avoid these charges is the creation of service overlays, for example, a multimedia broadcast onto a unicast cellular service [1]-[3] based on the so-called superposition coding [4], [5]. In conventional time or frequency division multiplexing, each service uses only a portion of the entire band, so that the rate of service is effectively halved. However, with superposition coding, the supported rate of each service is not necessarily halved since both the unicast and the broadcast signal overlap are transmitted through the same band. The problem is that they may interfere with each other, which makes the successive interference cancellation technique a key factor for the practical implementation of superposition coding. Other practical applications of superposition coding can also be found in [6]-[8], such as for unequal error protection and/or multi-rate transmission of broadcast traffic. Another class of overlaid transmission is that in [9]-[15], where, instead of superposition coding, a watermarking technique was considered for transmitter identification and later extended to an auxiliary data transmission over the existing TV broadcast, such as DVB [16] and the Advanced Television Systems Committee (ATSC) standard. Watermarking differs from the superposition coding in that its signal is just considered as ambient noise and the

interference cancellation technique is not used.

In this paper, we consider a service overlay where a spread spectrum (SS)-based add-on service is superimposed on the existing terrestrial Digital Multimedia Broadcasting (T-DMB) service [17]-[19], which is technically more similar to the watermarking technique for auxiliary data service [15] than to the superposition coding. Its primary application would be a low-rate emergency broadcast service. The fundamental requirements are as follows.

- 1) Overlaying an add-on service must not require any changes in the operation of the existing services.
- 2) The existing service must incur as little performance degradation as possible, if any, (for example, less than a few percentage points of coverage reduction).
- 3) The add-on service preferably has higher coverage than the existing service.

The first requirement makes it unfeasible to employ the successive interference cancellation and, hence, unlike the systems in [1]-[3] and [6]-[8], the overlaid system here must be operating independently; that is, the two signals are demodulated and decoded separately at the receiver, as in a watermarking technique, where they both act as interference with each other. For the first and second requirements, the relative power of the add-on service must be very small. A good option for reliable communication in this case would be an SS-based transmission, as in [9]-[15], where the tradeoff between rate and coverage can easily be controlled through the spreading factor. In view of the third requirement, an overlay with a spread spectrum signaling would be more suitable for a low-rate emergency service than serving over a separate band, which could be very narrow and subject to fading. One advantage of spread spectrum transmission over narrow band direct modulation is that use of the rake structure and diversity combining can mitigate multipath fading. Although it requires much wider transmission bandwidth, it is not a problem since the bandwidth here bears no cost when the signal is overlaid on the existing T-DMB band.

The key design parameters in the overlaid system under consideration would be the power ratio between the two service signals and the spreading factor of the add-on SS signal. The primary performance criteria would meanwhile be the coverage (or outage) of the two services and the rate of the add-on service (the rate of T-DMB service is assumed to be fixed). Hence, the objective in this paper is to explore the relation between the design parameters and the performance criteria and to find an affordable region for the desired service requirements. This will certainly be different from those in [20] and [21], where the objective is to maximize the overall throughput. However, in our problem, we consider fixed rate

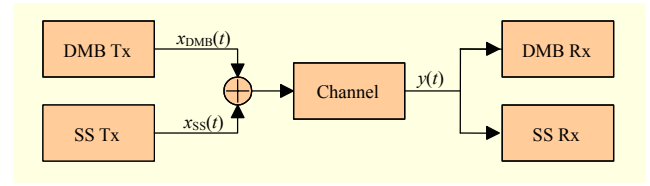


Fig. 1. Simplified system model under consideration.

broadcast services whose primary performance criterion is coverage, and the objective of power allocation is then to find the power ratio for an acceptable coverage reduction (for example, a few percentage points) in the existing service. Although the idea of an overlaid broadcast system is not new, the analytical approach and the results provided in this paper have not been studied before, and we believe that they can provide system developers and service providers with insight into the system behavior and can be used as a reference regarding system performance.

II. System Description and Performance Criteria

A simplified system structure is shown in Fig. 1, where the signals from the DMB transmitter and the SS transmitter are added and transmitted through the channel. At the receiver, the received signal is fed to the DMB and SS receivers, respectively, and demodulated separately. This means the DMB and SS signals act as interference to each other.

The two key parameters of the overlaid system are the power ratio between the two broadcast signals, that is, DMB to SS power ratio, α , and the spreading factor, N , of the SS signal, which are defined respectively as

$$\alpha = P_{\text{DMB}} / P_{\text{SS}} \quad (1)$$

$$N = R_c / R_{\text{SS}}, \quad (2)$$

where P_{DMB} and P_{SS} are the transmission power of the DMB and SS signals, respectively, and R_c and R_{SS} are the chip rate and data symbol rate of the SS signal, respectively. We also define the normalized bandwidth of the DMB and SS signals normalized to the sampling rate, R_s , as w_{DMB} and w_{SS} , which are given respectively by

$$w_{\text{DMB}} = \frac{W_{\text{DMB}}}{R_s} = \frac{N_{\text{used}}}{N_{\text{FFT}}}, \quad w_{\text{SS}} = \frac{R_c}{R_s}, \quad (3)$$

where R_s is the sampling rate that is common to the DMB and SS receivers, W_{DMB} is the nominal bandwidth of the DMB signal, and N_{FFT} and N_{used} are respectively the FFT point and the number of the DMB subcarriers used. Assuming the use of a raised cosine filter for the pulse shaping of the SS signal, we may set

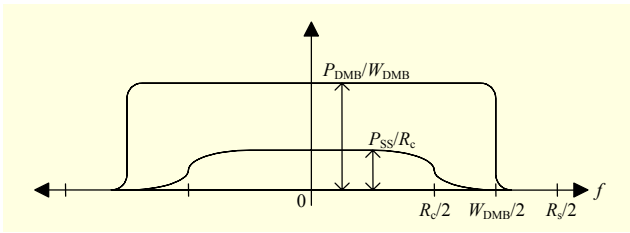


Fig. 2. Example power spectral densities of DMB and SS signal.

$$W_{\text{DMB}} \geq (1 + \eta) \cdot R_c, \quad (4)$$

where η is the roll-off factor of the pulse shaping filter. For implementation simplicity, it is recommended to set $R_s = mR_c$ for some integer m so that the DMB and SS receivers share one analog-to-digital converter. Figure 2 shows a sample power spectrum with $R_s = 2R_c = 2.048$ Msps, $W_{\text{DMB}} = 1.536$ MHz, and $\eta = 0.5$.

The primary figures of merit of the overlaid system would be the coverage of the DMB and SS-based add-on services defined respectively as

$$U_{\text{DMB}}(\alpha, D, \bar{\gamma}_{\text{DMB}}) \equiv E_{A(D)}[\Pr\{\gamma_{\text{DMB}}(\alpha) \geq \bar{\gamma}_{\text{DMB}}\}] \quad (5)$$

$$U_{\text{SS}}(\alpha, D, \bar{\gamma}_{\text{SS}}, N) \equiv E_{A(D)}[\Pr\{\gamma_{\text{SS}}(\alpha, N) \geq \bar{\gamma}_{\text{SS}}\}], \quad (6)$$

and the data rate of the SS-based add-on service, $R_{\text{SS}}(\bar{\gamma}_{\text{SS}}, N)$, limited by

$$R_{\text{SS}}(\bar{\gamma}_{\text{SS}}, N) \leq \frac{R_c}{N} \log_2(1 + \bar{\gamma}_{\text{SS}}) = C_{\text{SS}}(\bar{\gamma}_{\text{SS}}, N), \quad (7)$$

where $\bar{\gamma}_{\text{DMB}}$ and $\bar{\gamma}_{\text{SS}}$ are the minimum required signal-to-interference ratio (SINR) of DMB and SS, respectively, $A(D)$ is a circular area of radius D , and $E_{A(D)}[\cdot]$ represents an average over an area A . The ‘‘effective SINRs’’ at the DMB and SS receivers are $\gamma_{\text{DMB}}(\alpha)$ and $\gamma_{\text{SS}}(\alpha, N)$, respectively, to be discussed later.

III. Channel and Analytical Model

In this section, we consider an analytical model to explore the relation between the performance criteria and the system design parameters defined in the previous section. To do so, we need a large-scale path loss model and a small-scale fading channel model. The former is typically characterized by location dependence and log-normal shadowing and used to determine the received signal power and signal-to-noise ratio (SNR) in an average sense, while the latter is characterized by a power-delay profile and used to obtain the effective SINR and the bit error rate (BER) to finally measure the system-level performances, such as throughput and/or coverage. Reference [22] provides a system-level performance evaluation methodology.

1. Channel and Signal Model

A. Large-Scale Path Loss Model

First, define $P_r(r)$ as the received signal power measured at a receiver separated from the transmitter by a distance, r . Using the simplest path loss model [23], $P_r(r)$ is given in dB-scale by

$$P_{r,\text{dBm}}(r) = P_{t,\text{dBm}} - L_{0,\text{dB}} - 10n \log r + X_{\text{dB}}, \quad (8)$$

where n is the path loss exponent, X_{dB} is the log-normal shadowing that is assumed to be the Gaussian random variable with mean 0 and variance σ_{dB}^2 , $L_{0,\text{dB}}$ is the reference path loss, and $P_{t,\text{dBm}}$ and $P_{r,\text{dBm}}(r)$ are the transmission power and the received signal power, respectively, in dBm. We also define $\beta(r)$ as the corresponding SNR given by $\beta(r) = P_r(r)/\sigma^2$ with σ^2 being the noise power in mW. Using (8) and $N_{\text{dBm}} = 10 \cdot \log(\sigma^2)$, we have

$$\beta_{\text{dB}}(r) = P_{r,\text{dBm}}(r) - N_{\text{dBm}} = \bar{\beta}_{\text{dB}}(r) + X_{\text{dB}}, \quad (9)$$

where

$$\bar{\beta}_{\text{dB}}(r) = P_{t,\text{dBm}} - N_{\text{dBm}} - L_{0,\text{dB}} - 10n \log r. \quad (10)$$

Note from (9) that $\beta(r)$ has log-normal distribution, that is, its logarithm is a Gaussian random variable, such that

$$\beta_{\text{dB}}(r) \sim \mathcal{N}(\bar{\beta}_{\text{dB}}(r), \sigma_{\text{dB}}^2), \quad (11)$$

where $\mathcal{N}(a,b)$ represents the Gaussian density function with mean a and variance b .

B. Small-Scale Fading Channel Model

The small-scale fading channel model takes into account the multipath propagation and mobility. However, to make the analysis simple, we consider only the multipath propagation. In this case, the channel is characterized by a discrete time impulse response, h_k for $k = 0, 1, \dots, L-1$, where L is the channel length and each path gain is modeled as an independent Rayleigh distributed random variable with a normalizing condition

$$\sum_{l=0}^{L-1} |h_l|^2 = 1. \quad (12)$$

Typically, the condition is given by

$$\sum_{l=0}^{L-1} E |h_l|^2 = 1.$$

However, with the condition in (12), we can take into account only the impact of frequency selectivity without altering the average received power that, in our system model, is taken into account in the log-normal shadowing in (9).

C. Signal Model

Based on the channel model defined, the received signal

sampled at a rate, R_s , is represented as

$$y_k = \sqrt{P_r(r)} \cdot h_k^* (x_{\text{DMB},k} + x_{\text{SS},k}) + n_k, \quad (13)$$

where y_k is the received signal, n_k the Gaussian noise with mean 0 and $E[n_k n_{k-n}^*] = \sigma^2 \delta_n$ (δ_n is the Kronecker delta function), and $x_{\text{DMB},k}$ and $x_{\text{SS},k}$ are the DMB and the superimposed SS signals, respectively. In (13), the transmission power of the DMB and SS signals are defined respectively as

$$P_{\text{DMB}} = E |x_{\text{DMB},k}|^2, \\ P_{\text{SS}} = E |x_{\text{SS},k}|^2, \quad (14)$$

$$\text{with } P_{\text{DMB}} + P_{\text{SS}} = 1.$$

Although the total transmission power can be set arbitrarily, we already put this into the large-scale channel gain, that is, in (8), and we interpret P_{DMB} and P_{SS} as the portion of DMB and SS signal power in the total transmission power. Then, from the definition of α in (1), we have

$$P_{\text{DMB}} = \alpha / (1 + \alpha) \\ P_{\text{SS}} = 1 / (1 + \alpha).$$

D. Average SNR

Defining the received signals of DMB and SS respectively as $t_{\text{DMB},k} = \sqrt{P_r(r)} \cdot h_k^* x_{\text{DMB},k}$ and $t_{\text{SS},k} = \sqrt{P_r(r)} \cdot h_k^* x_{\text{SS},k}$, the received SNR (in an average sense) is given by

$$\beta(r) = \frac{E |t_{\text{DMB},k}|^2 + E |t_{\text{SS},k}|^2}{\sigma^2}$$

with

$$E |t_{\text{DMB},k}|^2 = P_r(r) \cdot \left(\sum_{l=0}^{L-1} |h_l|^2 \right) \cdot P_{\text{DMB}} = P_r(r) \cdot P_{\text{DMB}} \quad (15)$$

$$E |t_{\text{SS},k}|^2 = P_r(r) \cdot \left(\sum_{l=0}^{L-1} |h_l|^2 \right) \cdot P_{\text{SS}} = P_r(r) \cdot P_{\text{SS}}, \quad (16)$$

where we assume that each sample of $x_{\text{DMB},k}$ and $x_{\text{SS},k}$ are uncorrelated to each other, even though this may not be the case, especially when the samples in (13) are oversampled. For analytical simplicity, however, we will hold this assumption simply by assuming that each path in the channel impulse response has larger separation than the symbol duration of DMB and SS. Then, using (15) and (16), the received SNR becomes

$$\beta(r) = \frac{P_r(r)}{\sigma^2}, \quad (17)$$

as we previously defined.

2. Simple Analytical Model

In this subsection, we provide a simple analytical model without considering the multipath fading and the detailed modem structure. Although this assumption is extremely simplified, the results and their tendencies can give us insight into the actual system behavior.

Let $U(c, D)$ be the percentage of useful service area (over a circular area, A , of radius D) where the received SNR, $\beta_{\text{dB}}(r)$, in dB-scale is, over a threshold, c . According to [23], $U(c, D)$ can then be defined as

$$U(c, D) = E_{A(D)} [\Pr \{ \beta_{\text{dB}}(r) \geq c \}] \\ = \frac{1}{\pi D^2} \int_0^{2\pi} \int_0^D \Pr \{ \beta_{\text{dB}}(r) \geq c \} \cdot r dr d\theta. \quad (18)$$

For the arbitrary distribution of $\beta_{\text{dB}}(r)$, it is quite difficult to evaluate (18). Fortunately, however, one can obtain a closed form solution using the large-scale channel model in the previous subsection, that is, with the log-normal distribution in (11); for example, we obtain

$$\Pr \{ \beta_{\text{dB}}(r) \geq c \} = \frac{1}{2} \operatorname{erfc} \left(\frac{c - \bar{\beta}_{\text{dB}}(r)}{\sqrt{2} \sigma_{\text{dB}}} \right) \\ = \frac{1}{2} \operatorname{erfc} \left(a + b \ln \left(\frac{r}{D} \right) \right) \quad (19)$$

with

$$a = \frac{c - \bar{\beta}_{\text{dB}}(D)}{\sqrt{2} \sigma_{\text{dB}}}, \quad b = \frac{10n \log e}{\sqrt{2} \sigma_{\text{dB}}} = \frac{10 \log e}{\sqrt{2}} \cdot \frac{n}{\sigma_{\text{dB}}}$$

and, by plugging (19) into (18), we have [23]:

$$U(c, D) = \frac{1}{2} \left(\operatorname{erfc}(a) + \exp \left(\frac{1-2ab}{b^2} \right) \operatorname{erfc} \left(\frac{1-ab}{b} \right) \right). \quad (20)$$

Now, we evaluate the coverage of the DMB and SS services by using (20). Similar to the average SNR in (17), the SINR of DMB and SS signals in the average sense can be represented as

$$\gamma_{\text{DMB}}(r; \alpha) = \frac{1}{2.25} \cdot \frac{E |t_{\text{DMB},k}|^2}{E |t_{\text{DMB},k}|^2 + w_{\text{DMB}} \sigma^2} \\ = \frac{1}{2.25} \cdot \frac{P_r(r) P_{\text{DMB}}}{P_r(r) P_{\text{SS}} + w_{\text{DMB}} \sigma^2} \\ = \frac{1}{2.25} \cdot \frac{\alpha}{1 + (1 + \alpha) w_{\text{DMB}} \beta(r)^{-1}} \quad (21)$$

$$\gamma_{\text{SS}}(r; \alpha, N) = \frac{N \cdot E |t_{\text{SS},k}|^2}{w_{\text{SS}} (E |t_{\text{DMB},k}|^2 / w_{\text{DMB}} + \sigma^2)} \\ = \frac{NP_r(r) P_{\text{SS}}}{w_{\text{SS}} (P_r(r) P_{\text{DMB}} / w_{\text{DMB}} + \sigma^2)} \\ = \frac{N}{w_{\text{SS}} (\alpha / w_{\text{DMB}} + (1 + \alpha) \beta(r)^{-1})}, \quad (22)$$

where $\beta(r)$ is a log-normal random variable with mean $\bar{\beta}_{\text{dB}}(r)$ and variance σ_{dB}^2 . In (21), the SINR reduction by a factor of 1/2.25 (3.5 dB loss) is added taking differential quadrature phase-shift keying (DQPSK) modulation and non-coherent demodulation of the DMB signal [19]. This loss will be verified by a link-level simulation at the end of section IV. In (21) and (22), the SINRs were derived in the average sense; hence, with the condition in (12), the SINRs do not depend on the specific realization of the channel impulse response, h_k . Although this model is extremely simplified, it makes the problem simple, that is, using these simplified SINR, we can obtain the coverage of the DMB and SS services analytically as

$$\begin{aligned} U_{\text{DMB}}(\alpha, D, \bar{\gamma}_{\text{DMB}}) &= E_{A(D)} \left[\Pr \{ \gamma_{\text{DMB}}(\alpha) \geq \bar{\gamma}_{\text{DMB}} \} \right] \\ &= E_{A(D)} \left[\Pr \left\{ \beta \geq \frac{2.25 \cdot w_{\text{DMB}} \bar{\gamma}_{\text{DMB}} (1 + \alpha)}{\alpha - 2.25 \cdot \bar{\gamma}_{\text{DMB}}} \right\} \right] \\ &= U \left(10 \cdot \log \left(\frac{2.25 \cdot w_{\text{DMB}} \bar{\gamma}_{\text{DMB}} (1 + \alpha)}{\alpha - 2.25 \cdot \bar{\gamma}_{\text{DMB}}} \right), D \right) \end{aligned} \quad (23)$$

$$\begin{aligned} U_{\text{SS}}(\alpha, D, \bar{\gamma}_{\text{SS}}, N) &= E_{A(D)} \left[\Pr \{ \gamma_{\text{SS}}(\alpha, N) \geq \bar{\gamma}_{\text{SS}} \} \right] \\ &= E_{A(D)} \left[\Pr \left\{ \beta \geq \frac{w_{\text{DMB}} w_{\text{SS}} \bar{\gamma}_{\text{SS}} (1 + \alpha)}{N w_{\text{DMB}} - w_{\text{SS}} \bar{\gamma}_{\text{SS}} \alpha} \right\} \right] \\ &= U \left(10 \cdot \log \left(\frac{w_{\text{DMB}} w_{\text{SS}} \bar{\gamma}_{\text{SS}} (1 + \alpha)}{N w_{\text{DMB}} - w_{\text{SS}} \bar{\gamma}_{\text{SS}} \alpha} \right), D \right). \end{aligned} \quad (24)$$

Using (23), (24), and (7), we can explore the system behavior as a function of the system parameters, including the DMB to SS power ratio (α) and SS spreading factor (N). As noticed before, however, the frequency selectivity is not considered in the SINRs in (21) and (22), and the results may therefore vary from those using a more practical SINR model. Nevertheless, the analytical model in (23) and (24) can provide a quick view on the system behavior of the overlaid system, and its results can be used as references to verify the simulation results to be discussed in section V.

IV. Simulation Procedures

In section III.2, we obtained a closed form solution for the coverage of DMB and SS by using a simplified definition of the SINR without considering the specific realization of the channel impulse response. To obtain a more practical insight, we will now take the channel impulse response into account. In doing so, however, we cannot apply the analytical procedure outlined in section III.2. Instead, similar to the methodology in [22], we perform the simulation through the following steps.

Initialize:

1. Place transmitter at the center of a circular area $A(D)$.
2. Set $\bar{\gamma}_{\text{DMB}}$ and $\bar{\gamma}_{\text{SS}}$, respectively, to appropriate values.
3. Set α and N to some target values.

Loop:

1. Generate a random (receiver) location within the target area $A(D)$.
2. Use the model in (9) to set the average SNR, $\beta(r)$.
3. Generate a random channel impulse response, h_k for $k = 0, 1, \dots, L-1$, according to given power-delay profile.
4. Compute the effective SINR, $\gamma_{\text{DMB,eff}}(r; \alpha, h_k)$ and $\gamma_{\text{SS,eff}}(r; \alpha, N, h_k)$ for DMB and SS, respectively, using the procedure to be discussed shortly.
5. Compare it with the SINR threshold ($\bar{\gamma}_{\text{DMB}}$ and $\bar{\gamma}_{\text{SS}}$) and count the number of occurrences in which the effective SINR is higher than the threshold value.

Repeating Loop steps 1 through 5 many times, we can measure the coverage for given α and N . In (8) and (9), we defined the coverage as the probability that the received SINR is greater than some threshold; hence, in step 5, we count the number of occurrences where the effective SINR is higher than the threshold value. In fact, a more meaningful definition of coverage for a broadcast service would be the probability that the BER is less than a given threshold, say 10^{-4} . The BER, however, is quite difficult to evaluate analytically, especially when using channel coding. On the other hand, the SINR is much easier to analyze than BER, and, most of all, BER is a monotonically decreasing function of SINR so we need only find the SINR threshold corresponding to the BER threshold. In many cases, the SINR threshold is obtained by a link-level simulation for the given modulation and the coding scheme under consideration. It is a good approach for frequency flat channels since we need only perform the simulation for the additive white Gaussian noise (AWGN) channel. In frequency selective fading channels, however, the SINR threshold can be quite different for each realization of the channel impulse response or for different power-delay profiles, even if the average SINRs are the same. Especially in orthogonal frequency-division multiplexing (OFDM)-based systems, each data symbol is transmitted through a subcarrier of which the SNR may differ from those of other subcarriers. This makes it difficult to define a single SINR threshold for every realization of the channel impulse response. The notion of effective SNR mapping has been introduced to tackle this problem.

1. Effective SINR Mapping

Effective SNR mapping is a general term for link-level

performance approximation procedures that map an SINR or set of SINRs derived for a specific channel impulse response into an effective value at which the BER for the AWGN channel is approximately equal to the BER for the fading channel for a given (set of) SINR(s). It is extensively used in cellular system design, especially for the evaluation of system-level performances, such as cell throughput or outage. For spread spectrum signals, the effective SINR calculation in [22] is typically used, while the exponential effective SNR mapping (EESM) in [24], [25] is typical for OFDM-based systems. Here, we will use the one in [22] for the SS and the EESM in [24], [25] for the DMB, but with a slight modification. To evaluate the effective SINR, we need to take into account the demodulation procedure of both the DMB and the SS signals.

A. Effective SINR for SS Signal

Receivers for SS signals typically employ the rake structure, where multiple correlation receivers (so-called “fingers”) are used simultaneously (of which each one is assigned to each of those paths with relatively high path gain), and their outputs are maximal ratio combined. With this receiver structure, the SINR for any given channel impulse response, h_k , can be determined as follows: for the n -th path SS signal, $h_n x_{SS,k-n}$, all other signals are interference, such that, after despreading, the SINR for the n -th path signal is given by

$$\begin{aligned} \gamma_{SS, \text{finger}}^{(n)}(r; \alpha, N, h_k) &= \frac{N \cdot P_r(r) P_{SS} |h_n|^2}{P_r(r) P_{SS} \cdot \sum_{l \neq n} |h_l|^2 + E |n'_k|^2} \\ &= \frac{N \cdot P_r(r) P_{SS} |h_n|^2}{P_r(r) P_{SS} \cdot \sum_{l \neq n} |h_l|^2 + w_{SS} (P_r(r) P_{DMB} / w_{DMB} + \sigma^2)} \\ &= \frac{N |h_n|^2}{\sum_{l \neq n} |h_l|^2 + w_{SS} (\alpha / w_{DMB} + (1 + \alpha) \beta(r)^{-1})}. \end{aligned} \quad (25)$$

Applying the maximal ratio combining of the finger outputs, the SINR at the combiner output is then given by the sum of the respective SINRs [26]

$$\gamma_{SS, \text{MRC}}(r; \alpha, N, h_k) = \sum_{n \in \Phi} \gamma_{SS, \text{finger}}^{(n)}(r; \alpha, N, h_k), \quad (26)$$

where Φ is the set of indices of the paths with the highest signal amplitudes. Finally, the effective SINR is obtained by ceiling the SINR to a maximum value, γ_{\max} , [27], that is,

$$\gamma_{SS, \text{eff}}(r; \alpha, N, h_k) = \left(\gamma_{\max}^{-1} + \left(\gamma_{SS, \text{MRC}}(r; \alpha, N, h_k) \right)^{-1} \right)^{-1}. \quad (27)$$

B. Effective SINR for DMB Signal

One of the key features of T-DMB is that it is OFDM-based. The SINR should therefore also be evaluated in the frequency

domain, that is, per subcarrier SINR. Let H_m be the M -point discrete Fourier transform of h_k . With the condition in (12), we have $\sum_m |H_m|^2 = M$. Assuming the power spectrum of the SS signal is white within the bandwidth of the DMB signal¹⁾, the SINR for the m -th subcarrier is given by

$$\begin{aligned} \gamma_{DMB}^{(m)}(r; \alpha, h_k) &= \frac{1}{2.25} \cdot \frac{P_r(r) |H_m|^2 P_{DMB}}{P_r(r) |H_m|^2 P_{SS} + w_{DMB} \sigma^2} \\ &= \frac{1}{2.25} \cdot \frac{|H_m|^2 \alpha}{|H_m|^2 + (1 + \alpha) w_{DMB} \beta(r)^{-1}}, \end{aligned} \quad (28)$$

where the factor 1/2.25 implies the 3.5-dB loss due to the differential detection (see the next subsection). The SNR ceiling is then applied for each sub-subcarrier before evaluating the effective SINR mapping. Similar to SS, it is obtained by the harmonic sum with the maximum SNR, γ_{\max} , that is,

$$\tilde{\gamma}_{DMB}^{(m)}(r; \alpha, h_k) = \left(\gamma_{\max}^{-1} + \left(\gamma_{DMB}^{(m)}(r; \alpha, h_k) \right)^{-1} \right)^{-1}. \quad (29)$$

These per-subcarrier SINRs are finally mapped to a single effective SINR value by using the exponential effective SNR mapping (EESM) in [24], [25]

$$\begin{aligned} \gamma_{DMB, \text{eff}}(r; \alpha, h_k) &= -\frac{1}{\rho} \log \left(\frac{1}{|\Psi|} \sum_{m \in \Psi} \exp \left(-\rho \cdot \tilde{\gamma}_{DMB}^{(m)}(r; \alpha, h_k) \right) \right), \end{aligned} \quad (30)$$

where Ψ is the set of subcarrier indices used, and ρ is the mapping parameter. Generally, ρ must be chosen depending on the modulation size and the channel coding scheme used. For example, a suitable choice for QPSK and channel coding of rate 1/2 is 1.56 [28].

2. SINR Thresholds

In digital broadcast service, quality of service (QoS) is often measured by BER, which monotonically decreases with SINR, and a sustainable BER that ensures a certain level of QoS is defined for specific service, for example, 10^{-4} BER for audio and 10^{-6} for video. Recalling that the effective SINR is an effective value at which the BER for the AWGN channel is approximately equal to the BER for the multipath fading channel with a specific channel impulse response, the remaining task is to determine appropriate SINR thresholds, $\bar{\gamma}_{DMB}$ and $\bar{\gamma}_{SS}$, that are minimally required to obtain the sustainable BER, by performing link-level simulations for the AWGN channel. To do so, we need to define the modulation and coding scheme used for the DMB and SS signals, respectively. To be specific, the modulations of the DMB and

¹⁾ Although it is practically not as shown in Fig.2, we assume this for analytical simplicity.

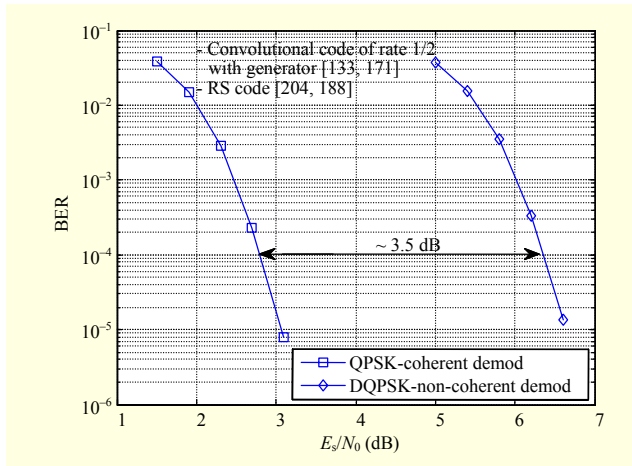


Fig. 3. BER performance of concatenated convolutional/RS code of terrestrial DMB, with QPSK and DQPSK modulation, respectively; WGN channel, 8-bit quantization applied to demodulator output before fed to Viterbi decoder.

SS services are assumed to use DQPSK and QPSK, respectively, and the same channel coding of the concatenated convolutional code (of rate 1/2) and Reed-Solomon (RS) code as defined in the terrestrial DMB layer 1 specification [19]. With these modulations and the coding scheme, we perform a link-level simulation to evaluate the BER performance in an AWGN channel environment.

The results are shown in Fig. 3. Note that the SINR threshold for 10^{-4} BER is slightly less than 3 dB for QPSK and coherent demodulation, while, for DQPSK modulation and non-coherent demodulation as in DMB, there is approximately 3.5-dB SNR loss from the performance of QPSK modulation with coherent demodulation. Since this loss is already taken into account in the computation of the effective SINR in (21) and (28), we set the SINR thresholds for both DMB and SS to 3 dB, that is, $\bar{\gamma}_{\text{DMB}} = \bar{\gamma}_{\text{SS}} = 3$ dB, also taking a certain margin into account. These values will be used in the simulation discussed in the next section.

V. Simulation Results

1. Simulation Setting

Following the procedure summarized in the previous section, we perform simulations to evaluate the coverage of the DMB and the SS and the tradeoff behavior between coverage and rate in the SS system. The parameters used in the simulation are summarized in Table 1, where the sampling rate, R_s , is set to 2.048 Msps, which is the minimum sampling rate for DMB signal reception. Although an oversampling is typical, we use the minimum value to simplify the analysis and simulation.

For the large-scale path loss, we applied the Hata model for

Table 1. Channel/system parameters used for simple analysis.

Parameter	Value
$P_{t,\text{dBm}}$	60 dBm (1 kW)
N_0	-175 dBm/Hz
$W = R_s$	2.048 MHz
$L_{0,\text{dB}}$	97 dB
σ_{dB}	8 dB
n	3
w_{DMB}	0.75
$w_{\text{SS}} (\eta)$	0.5 (0.5)
Antenna gain (receiver)	6 dB
Noise figure (NF_{dB})	9 dB
$N_{\text{dBm}} = N_0[\text{dBm}] + 10 \log_{10} W + NF_{\text{dB}}$	

urban areas [23], in which the path loss is given by

$$L(r) = 69.55 + 26.16 \log f - 13.82 \log h_T - a(h_R) + [44.9 - 6.55 \log h_T] \log r \quad (31)$$

with

$$a(h_R) = 8.29(\log(1.54 \cdot h_R))^2 - 1.1 \quad \text{for } f \leq 300 \text{ MHz},$$

where f is the carrier frequency in MHz, h_T and h_R are the height in m (antenna elevation) of the transmitter and the receiver, respectively, and r is the distance in km between the transmitter and the receiver. By equating (31) with the path loss in (8), we identify

$$L_{0,\text{dB}} = 69.55 + 26.16 \log f - 13.82 \log h_T - a(h_R)$$

$$n = [44.9 - 6.55 \log h_T] / 10.$$

Specifically, we choose $f = 200$ MHz, the DMB frequency in Korea, $h_T = 200$, assuming the transmitter is installed on top of a city side mountain, and $h_R = 2$. With these values, we obtain $L_{0,\text{dB}} \approx 97$ and $n = 3$ as shown in Table 1. The standard deviation of the log-normal shadowing, σ_{dB} , is set to 8 dB, which is a typical value for urban areas [23]. For the small-scale fading channel model, we use an SUI-5 model, which is defined by a 3-path exponential power-delay profile with the power (0, 5, 10) dB and the delay (0, 5, 10) μs .

2. Simulation Results

Figure 4 shows the cumulative distribution function (CDF) of the effective SINR of the DMB, which is equivalent to the outage performance, that is, $1 - U_{\text{DMB}}(\alpha, D, \bar{\gamma}_{\text{DMB}})$, plotted as a function of $\bar{\gamma}_{\text{DMB}} = X$. Note that the outage performance

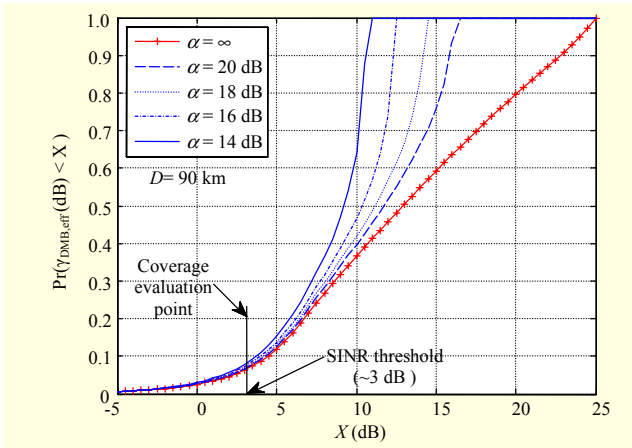


Fig. 4. CDF of effective SINR of DMB; $D = 90$ km, $\alpha = \infty, 20, 18, 16,$ and 14 dB, respectively, where $\alpha = \infty$ represents DMB only system.

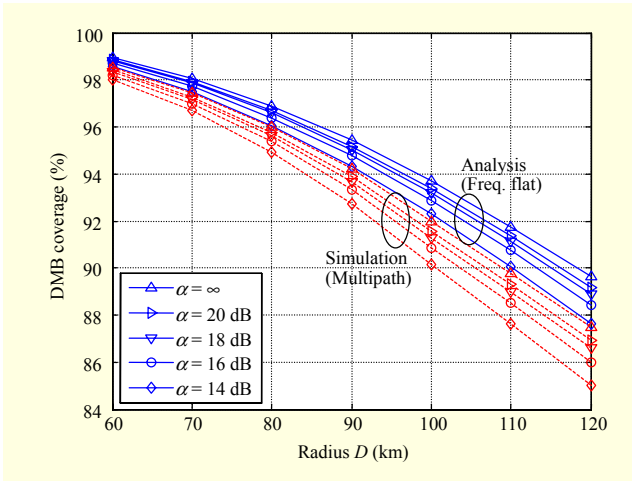


Fig. 5. DMB coverage $U_{\text{DMB}}(\alpha, D, \bar{\gamma}_{\text{DMB}})$ as function of radius D ; $\bar{\gamma}_{\text{DMB}} = 3$ dB, $\alpha = \infty, 20, 18, 16,$ and 14 dB, respectively.

degradation is considerable in high-SINR regions, for example, for $X > 10$ dB, while it is not for $X < 5$ dB. In high-SINR regions, where background noise power is very small, the SS signal degrades the DMB performance quite a bit, even with a low power level of the SS signal, which, however, is stronger than the background noise. In small-SINR regions (for example, $X < 5$ dB), the degradation is meanwhile much smaller than in high-SINR regions because the background noise power is now much stronger than the interference (that is, SS) power such that $P_r(r)P_{\text{SS}} \ll \sigma^2$. Note also that the effective SINR reduction in high-SINR regions is not a problem since the quality of the DMB broadcast service will still be satisfactory once the effective SINR is over the 3-dB SINR threshold.

Figure 5 shows the coverage of the DMB service for a circular area A of radius D , which is equivalent to the CDF

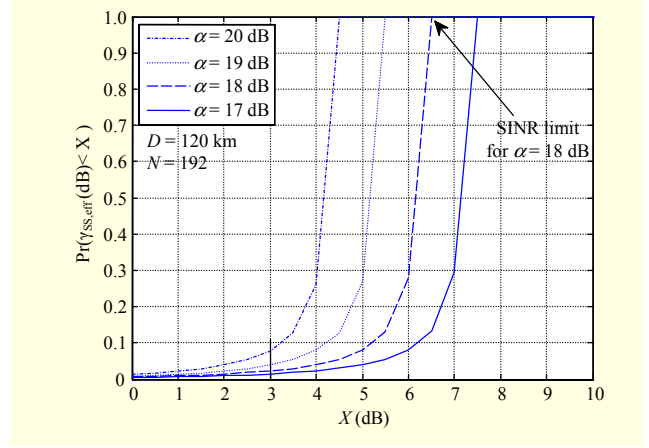


Fig. 6. CDF of effective SINR of SS; $D = 120$ km, $N = 192$, $\alpha = 20, 19, 18$ and 17 dB, respectively.

evaluated at $X = 3$ dB in Fig. 4. We plot both the analytical results obtained by (23) and the simulation results obtained by the procedure in the previous section. The difference between the analytical and simulation results stems from the fact that, in analysis, we do not consider the frequency selectivity, while we use the EESM in the simulation to take the multipath fading into account. This results in a further reduction of the effective SINR and the coverage performance. Compared to the coverage of the DMB-only system, the coverage reduction in the overlaid system is less than 1% for a high DMB to SS power ratio, say $\alpha > 18$ dB.

Similar to Fig. 4 for DMB, Fig. 6 shows the CDF of the effective SINR of the SS service, which is equivalent to the SS outage performance, $1 - U_{\text{SS}}(\alpha, D, \bar{\gamma}_{\text{SS}})$, plotted as a function of $\bar{\gamma}_{\text{SS}} = X$. For DMB, the coverage performance can be controlled solely by α while, for SS, the coverage can also be controlled by the spreading factor, N ; that is, the SINR is improved with a larger value of N , which happens of course at the expense of the SS service rate, which is inversely proportional to N as shown in (7). Note that the effective SINR is limited by N/α , that is, from (25), we have for $\beta(r) \rightarrow \infty$ and sufficiently large N and α

$$\gamma_{\text{SS,finger}}^{(n)}(r; \alpha, N, h_k) \rightarrow \frac{w_{\text{DMB}} N |h_n|^2}{w_{\text{SS}} \alpha},$$

such that, with (26),

$$\gamma_{\text{SS,MRC}}(r; \alpha, N, h_k) \approx \frac{w_{\text{DMB}} N}{w_{\text{SS}} \alpha} \left[\sum_{n \in \Phi} |h_n|^2 \right] = \frac{w_{\text{DMB}} N}{w_{\text{SS}} \alpha},$$

assuming all the paths are maximal ratio combined. By using $w_{\text{DMB}}/w_{\text{SS}} = 0.75/0.5$ (≈ 1.7 dB), $N = 192$ (≈ 22.8 dB), and $\alpha = 18$ dB, we approximately obtain the SINR limit marked in the figure, which is slightly smaller than $w_{\text{DMB}} N/w_{\text{SS}} \alpha \approx 6.5$ dB, due to the SINR ceiling in (27).

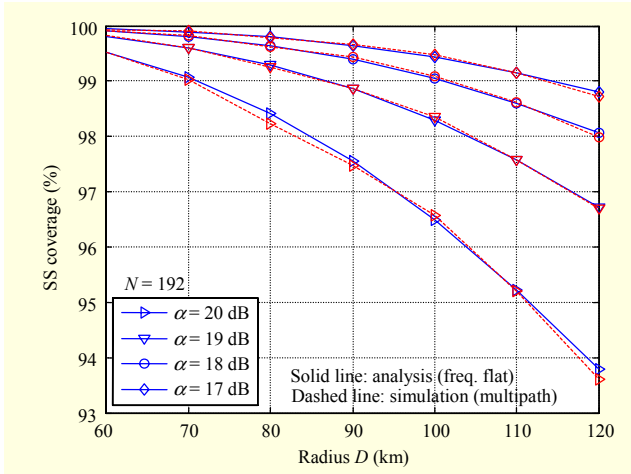


Fig. 7. SS coverage $U_{SS}(\alpha, D, \bar{\gamma}_{SS}, N)$ as function of radius D ; $\bar{\gamma}_{SS} = 3$ dB, $\alpha = 20, 19, 18$, and 17 dB, respectively.

Figure 7 shows the coverage of the SS-based add-on service for a circular area A of radius D , which is equivalent to the CDF evaluated at $X = 3$ dB in Fig. 6. We also plot both the analytical results obtained by (24) and the simulation results obtained through the procedure in the previous section. Unlike the DMB coverage in Fig. 5, the analytical results are quite close to the simulation results. Comparing (24) with (26), we realize that the only difference is the self-interference (that is, the interference from the delayed version of the transmitted SS signal) added in the denominator in (25). Noting that this self-interference can be ignored with sufficiently large N , it can be easily verified by inserting (25) into (26) to obtain

$$\begin{aligned} & \gamma_{SS, \text{MRC}}(r; \alpha, N, h_k) \\ &= \sum_{n \in \Phi} \left(\frac{N |h_n|^2}{\sum_{l \neq n} |h_l|^2 + w_{SS}(\alpha / w_{\text{DMB}} + (1 + \alpha)\beta(r)^{-1})} \right) \\ & \approx \frac{N \left(\sum_{n \in \Phi} |h_n|^2 \right)}{w_{SS}(\alpha / w_{\text{DMB}} + (1 + \alpha)\beta(r)^{-1})}, \end{aligned}$$

which is equal to (24), assuming all the paths are maximal ratio combined. Note that the coverage of the SS service can be made arbitrarily close to 100% by increasing N at the cost of the service rate reduction shown in (7). Now, the question is what the trade rate between the two performance measures is.

Figure 8 shows the tradeoff between the coverage and the rate for the SS-based add-on service, that is, $U_{SS}(\alpha, D, \bar{\gamma}_{SS}, N)$ versus $C_{SS, \text{Max}}(\bar{\gamma}_{SS}, N)$, with different values of radius D . We set $\alpha = 18$ dB. Once we fix the service area, the maximum service rate is limited by the target coverage specified by the service requirement. With these results, we estimate that the possible rate of the add-on service would be 10 kbps to 20 kbps,

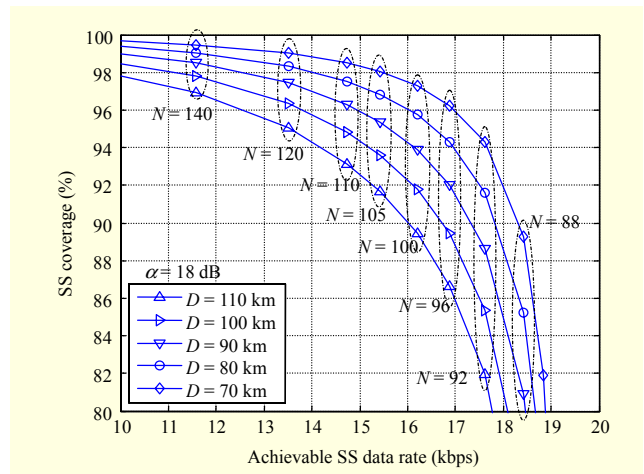


Fig. 8. Tradeoff between coverage and rate in SS based service, that is, $U_{SS}(\alpha, D, \bar{\gamma}_{SS}, N)$ versus $C_{SS, \text{Max}}(\bar{\gamma}_{SS})$ with different radius D ; $\bar{\gamma}_{SS} = 3$ dB, $\alpha = 18$ dB.

which seems to be sufficient for text messages and a compressed voice/audio.

VI. Concluding Remarks

In this paper, we considered an overlaid broadcast service where an SS-based broadcast signal is overlaid onto the existing T-DMB service. Using a simple analysis and simulation procedure modified from the one developed for cellular system design in 3GPP, we investigated the relation between the key system design parameters, that is, the DMB to SS power ratio and the SS spreading factor, and the primary performance measures, such as the coverage of DMB and SS and the achievable SS service rate. Based on the simulation results, we found that a low-rate SS-based add-on service can co-exist with the T-DMB service with a marginal degradation in DMB coverage (1% or less). As a matter of fact, such coverage reduction in DMB service can be made arbitrarily small by increasing the SS spreading factor, that is, at the cost of the SS service rate. However, there might be other solutions to compensate for the DMB coverage reduction, for example, by slightly increasing the repeater transmission power. Providers of T-DMB services in Korea currently deploy many repeaters to fill the shadow region. Although we did not consider repeaters in our simulation, it can easily be inferred that the coverage reduction in DMB service will occur around the edge of those shadow regions. This means that the average SNR, β , can be improved by only slightly increasing the repeater transmission power so that the “slight” coverage reduction can be compensated to a level that could be obtained in the DMB-only system.

References

- [1] F. Khan, "Broadcast Overlay on Unicast via Superposition Coding and Interference Cancellation," *Proc. VTC*, vol. 2, Montreal, Canada, Sept. 2006, pp. 836-841.
- [2] D. Kim et al., "Superposition of Broadcast and Unicast in Wireless Cellular Systems," *IEEE Commun. Mag.*, vol. 46, no. 7, July 2008, pp. 110-117.
- [3] S. Yoon and D. Kim, "Performance of Superposition Coded Broadcast/Unicast Service Overlay System," *IEICE Trans. Commun.*, vol. 91B, no. 9, Sept. 2008, pp. 2933-2939.
- [4] T.M. Cover and J.A. Thomas, *Elements of Information Theory*, New York: Wiley Interscience, 1991.
- [5] T.M. Cover, "Broadcast Channels," *IEEE Trans. Inf. Theory*, vol. 18, no. 1, Jan. 1972, pp. 2-14.
- [6] T.W. Sun et al., "Superposition Turbo TCM for Multi-Rate Broadcast," *Proc. ICC*, May 2003, pp. 3145-3149.
- [7] X. Wang and M.T. Orchard, "Design of Superposition-Coded Modulation for Unequal Protection," *Proc. ICC*, June 2001, pp. 412-416.
- [8] S. Gadkari and K. Rose, "Time Division versus Superposition Coded Modulation Schemes for Unequal Error Protection," *IEEE Trans. Commun.*, vol. 47, no. 3, Mar. 1999, pp. 370-379.
- [9] X. Wang, Y. Wu, and B. Caron, "Transmitter Identification Using Embedded Pseudo Random Sequences," *IEEE Trans. Broadcast.*, vol. 50, no. 3, 2004, pp. 244-252.
- [10] X. Wang, Y. Wu, and J.-Y. Chouinard, "Robust Data Transmission Using the Transmitter Identification Sequences in ATSC DTV Signals," *IEEE Trans. Consum. Electron.*, vol. 51, no. 1, 2005, pp. 41-47.
- [11] F. Yang et al., "Transmitter Identification with Watermark Signal in DVB-H Signal Frequency Network," *IEEE Trans. Broadcast.*, vol. 55, no. 3, 2009, pp. 663-667.
- [12] S.I. Park et al., "Transmitter Identification Signal Analyzer for Single Frequency Network," *IEEE Trans. Broadcast.*, vol. 54, no. 3, Part: 1, 2008, pp. 383-393.
- [13] S.I. Park et al., "RF Watermark Backward Compatibility Tests for the ATSC Terrestrial DTV Receivers," *IEEE Trans. Broadcast.*, vol. 57, no. 2, Part: 1, 2011, pp. 246-252.
- [14] S.I. Park, H.M. Kim, and W. Oh, "Reception Power Estimation Using Transmitter Identification Signal for Single Frequency Network," *IEEE Trans. Broadcast.*, vol. 55, no. 3, 2009, pp. 652-655.
- [15] Y.-W. Suh et al., "A Novel TxID Insertion System for ATSC DTV Auxiliary Data Transmission," *IEEE Trans. Consum. Electron.*, vol. 57, no. 1, 2011, p. 35.
- [16] ETSI "Digital Video Broadcasting (DVB): Transmission System for Handheld Terminals," ETSI EN 302 304 v1.1.1, Nov. 2004.
- [17] S. Cho et al., "System and Services of Terrestrial Digital Multimedia Broadcasting (T-DMB)," *IEEE Trans. Broadcast.*, vol. 53, no. 1, Mar. 2007, pp. 171-178.
- [18] G. Lee et al., "Development of Terrestrial DMB Transmission System based on Eureka-147 DAB System," *IEEE Trans. Consum. Electron.*, vol. 51, no. 1, Feb. 2005, pp. 63-68.
- [19] ETSI, "Radio Broadcasting Systems; Digital Audio Broadcasting (DAB) to Mobile, Portable and Fixed Receivers," ETSI EN 300 401 ver. 1.3.3, May 2001.
- [20] F. Etemadi and H. Jafarkhani, "Optimal Rate and Power Allocation for Layered Transmission with Superposition Coding," *Proc. Data Compression Conf.*, Mar. 27-29, 2007, p. 380.
- [21] Y. Liu et al., "Optimal Rate Allocation for Superposition Coding in Quasi-Static Fading Channels," *Proc. ISIT 2002*, Lausanne, Switzerland, June 30-July 5, 2002, p. 111.
- [22] 3GPP2 WG3, "1x EV-DO Evaluation Methodology," v1.3, Aug. 2003.
- [23] T.S. Rappaport, *Wireless Communications: Principles & Practice*, Upper Saddle River, NJ: Prentice Hall, Inc., 1996.
- [24] M. Lampe, H. Rohling, and J. Eichinger "PER-Prediction for Link Adaptation in OFDM Systems," *7th Int. OFDM Workshop*, Hamburg, Germany. Sept. 2002.
- [25] Y. Blankenship et al., "Link Error Prediction Methods for Multicarrier Systems," *Proc. VTC2004 Fall*, Los Angeles, 2004.
- [26] J.G. Proakis, *Digital Communications*, Boston: McGraw Hill, 1995.
- [27] 3GPP2 WG3, "Derivation of Equations Used in the Computation of Symbol SINR and Equivalent SNR for OFDM-Based Transmission," 3GPP2 Working Document C30-20040823-016, Aug. 2004.
- [28] 3GPP TSG-RAN, "Feasibility Study for Enhanced Uplink for UTRA," Technical Report TR25.892 v1.1.0, Mar. 2004.



Seokhyun Yoon received his BS and MS in electronics engineering from SungKyunKwan University, Suwon, Rep. of Korea, in 1992 and 1996, respectively, and his PhD in electrical and computer engineering from the New Jersey Institute of Technology (NJIT), Newark, NJ, USA, in 2003. In 1999, he was with ETRI, Daejeon, Rep. of Korea. From 2003 to 2005, he was with the Telecommunication R&D Center, Samsung Electronics Co., Ltd., Suwon, Rep. of Korea, where he worked on technologies for wireless/mobile air interfaces. Currently, he is an associate professor in the Department of Electronics Engineering, Dankook University, Yongin-si, Kyunggi-do, Rep. of Korea. His research activities are focused on wireless communications and signal processing for communications. Dr. Yoon was awarded the Hashimoto Prize in 2003 and the Haedong Best Paper Award in 2006.



Bo-mi Lim received her BS from Ajou University, Suwon, Rep. of Korea, in 2008 and her MS from the Korea Advanced Institute of Science and Technology (KAIST), Daejeon, Rep. of Korea, in 2010. Since 2010, she has been a member of the research staff in the Broadcasting System Research Department, ETRI, Daejeon, Rep. of Korea. She is currently working on a project to develop an emergency broadcast system based on T-DMB. Her research interests include wireless communication system design, MIMO signal processing, and digital broadcasting.



Yong Tae Lee received his BSEE and MSEE from Korea Aerospace University in 1993 and 1995, respectively. Since 1995, he has been with the Radio Signal Processing Department and Broadcasting System Research Department, ETRI, Daejeon, Rep. of Korea, where he is a principal researcher. He received his PhD from Yonsei University, Rep. of Korea, in 2007. Also, he is currently the project leader of development of the wake-up and emergency message transceiver technology for a T-DMB-based emergency broadcasting service. He is a member of IEEE and a member of the IEEE Transaction on Consumer Electronics Publications editorial board. In addition, he is a steering board member of the WorldDMB Forum. His research interests include digital signal processing and RF signal processing, in particular, signal processing for digital broadcasting systems and digital communication systems.